Effects of pH on the Cytotoxicity of Sodium Trioxodinitrate (Angeli's Salt)

Detcho A. Stoyanovsky,*,† Nina F. Schor,‡ Karen D. Nylander,‡ and Guy Salama§

Departments of Surgery, Pediatrics, Neurology, and Pharmacology, University of Pittsburgh, Pittsburgh, Pennsylvania 15213, Pediatric Center for Neuroscience, Children's Hospital of Pittsburgh, Pittsburgh, Pennsylvania 15213, and Cell Biology and Physiology, School of Medicine, University of Pittsburgh, A115 Scaife Hall, 3550 Terrace Street, Pittsburgh, Pennsylvania 15261

Received April 22, 2003

Tumor tissues have an acidic microenvironment with a pH from 6.0 to 7.0, whereas the intra- and extracellular milieu of normal cells is 7.4. We have found that the hydrolysis of sodium trioxodinitrate (Angeli's salt; **1**) to hydroxyl radical (•OH) was 10 times higher at pH = 6.0 than at pH = 7.4. It is hypothesized that the formation of •OH in solutions of **1** reflects the hydrolysis of the latter compound to nitroxyl (HNO) which dimerizes to *cis*-hyponitrous acid (HO−N=N−OH; **3**) with concomitant azo-type homolytic fission to N_2 and •OH. In weakly acidified solutions, **1** exhibited strong toxicity to cancer cells that was inhibited by scavengers of hydroxyl radical, whereas no toxicity was observed at pH = 7.4. In a subcutaneous xenograft model of pheochromocytoma, **1** markedly inhibited tumor growth at a dose that was nontoxic to nude mice. These data suggest that the H^+-amplified production of •OH from **1**, and maybe other precursors of HNO, could be a selective mechanism for destruction cells with an acidic intra- or extracellular microenvironment.

Introduction

Structural studies at the molecular level have focused on the design of anticancer drugs that do not have the limitations found with conventional drugs, such as the lack of selectivity for cancer cells and resistance phenomena. An ideal anticancer drug could be defined as a compound that is toxicologically inactive until metabolized by a molecular event unique to neoplastic cells. However, the identification of compounds that can be converted to toxic metabolites in response to a cancer-specific biochemical event remains a major challenge in the medicinal chemistry of cancer treatment.

A common feature of all cancer cells thus far examined is their metabolic anomaly of generating spontaneously an acidic extracellular milieu. The intense metabolism of glucose to lactic acid and the hydrolysis of ATP in hypoxic tumors lead to acidification in the microenvironment of cancer cells (reviewed in ref 1). In actively glycolyzing tumors, the extracellular pH is in the range of 6.0−7.0, whereas the extra- and intracellular milieu of most tissues has a pH of 7.4.[1−3] In some tumors, further decrease in extracellular pH can be stimulated by the administration of glucose or drugs that reduce blood flow to the area;[1−4] alternatively, the acidic environment of tumors has been efficiently neutralized by administration of $NaHCO_3$.[5] Tumor pH gradients have been shown to affect the cytotoxicity of some ionic anticancer drugs, because their nonionized forms are more lipophilic and cross cell membranes more efficiently than the deprotonated forms. This phenomenon leads to substantial differences in the distribution of such drugs between tumor and normal tissues, suggesting that the acidity of tumors can be utilized for the induction of cell-specific toxicity.[5,6]

In principle, metabolic activation of anticancer drugs to toxic species could be envisaged in the acidic extracellular environment of cancer cells. We recently reported that the hydrolysis of sodium trioxodinitrate (**1**; Angeli's salt; *N*-nitrohydroxylamine) leads to the formation of HNO and •OH, whereas maximal production of •OH was observed at pH = 5.0.[7] Due to its high reactivity, •OH is one of the most toxic species that can be formed in biological systems. When generated, •OH reacts with a neighboring molecule at first collision; thus, it cannot diffuse far from its site of generation, no further than the nearest molecules (diffusion-controlled reactions).[8] Hence, we hypothesized that **1** may exert selective toxicity to cancer cells via a mechanism that includes a pH-dependent, site-specific generation of •OH. To test this possibility, experiments were conducted for quantification of •OH formed in aqueous solutions of **1**, with an emphasis on the effects of pH on the cytotoxicity of this compound.

Results

EPR Analysis of the Hydrolysis of 1. In model studies aimed at mimicking the biochemistry of HNO, **1** is often used as a donor of this species. Depending on the degree of protonation, the stability of **1** in aqueous solutions follows the sequence $N_2O_3^{2-}$ (**1**) > $HN_2O_3^-$ (**1b**) > $H_2N_2O_3$ (**1a**, $pK_1 = 3.0$ and $pK_2 = 9.35$).[9] **1** is relatively stable in alkaline solutions (pH > 10). However, the rate of decomposition of **1b** within the pH interval 4−8 is rapid and $[H^+]$-independent and leads to the formation of HNO (Scheme 1).[9,10] In studies with $Na_2(O^{15}NNO_2)$, Bonner and Ravid demonstrated that hydrolytically generated $H^{15}NO$ dimerizes to *cis*-hyponitrous acid (**3**), which is unstable and decomposes to $^{15}N_2O$ and H_2O;[10] the decomposition of **3** is especially fast in aqueous

* Corresponding author. Phone: (412) 647-6087. FAX: (412) 647-5959. E-mail: stoyanovskyd@msx.upmc.edu.
† Department of Surgery, University of Pittsburgh.
‡ Departments of Pediatrics, Neurology, and Pharmacology, University of Pittsburgh, and Pediatric Center for Neuroscience, Children's Hospital of Pittsburgh.
§ Cell Biology and Physiology, School of Medicine, University of Pittsburgh.

10.1021/jm030192j CCC: $27.50
Published on Web 12/09/2003

Scheme 1

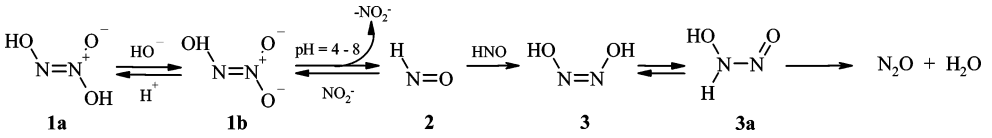

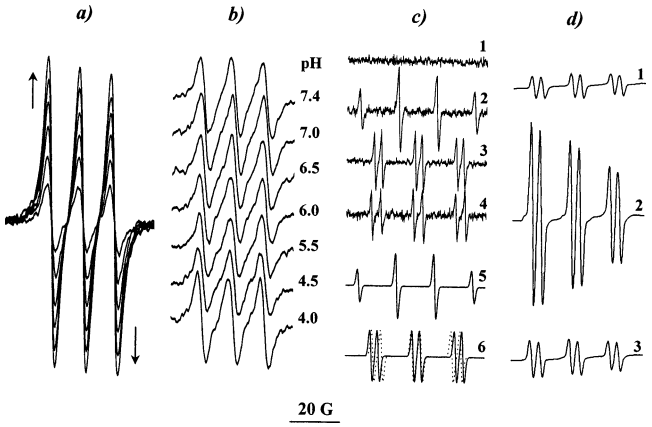

Figure 1. EPR spectra of **5**, **6**, **8**, and **10** formed in solutions of **1b**. EPR measurements and spectra simulations were performed as described in the Experimental Section. Reactions were carried out at 20 °C in either 0.1 M TRIS (a and b) or phosphate buffer (c and d; pH = 7.4). DMSO, DMPO, POBN, and PBN were used at concentrations of 0.2, 0.12, 0.10, and 0.05 M, respectively. (a) Time-course and effects of pH (b) on the formation of **6** (MGD, 1 mM; $FeCl_3$, 0.3 mM; **1b**, 0.1 mM). Before recording the spectra, the final reaction solutions were preincubated for 4 min. Arrows indicate the direction of time-dependent changes of the EPR spectra of **6**. Consecutive EPR spectra were recorded with a time interval of 4 min. (c) Spectrum 1, DMPO; spectrum 2, **1b** (1 mM) and DMPO; spectrum 3, POBN, DMSO, and **1b** (1 mM); spectrum 4, PBN, DMSO, and **1b** (1 mM); trace 5, computer simulation of the EPR spectrum of **5**; trace 6, computer simulation of the EPR spectra of **3** (solid lines) and **4** (dashed lines), respectively. (d) Effects of $K_3[Fe(CN)_6]$ on the EPR spectrum of **10** formed in solutions of **1b**. Spectrum 1, PBN, DMSO and **1b** (0.01 M; incubation time, 20 min); at $t = 24$ min, an addition of $K_3[Fe(CN)_6]$ (1 mM) was made and consecutive EPR spectra were recorded (spectra 2 and 3, respectively; $\Delta_{scan} = 4$ min).

solutions with pH = 6−13.[11] At pH < 4, the decomposition rate of **1a** increases with increasing acidity with production of NO•.[9] It has been reported that **1b** can trigger reactions of alkylation, condensation, and oxidation; the mechanism of these reactions, however, is not well-understood and cannot be correlated only with the hydrolysis **1b** to HNO.[12]

We have recently reported that **1b** can convert primary alcohols to aldehydes via the intermediate formation of •OH.[7] In these experiments, the formation of •OH was characterized by EPR spin-trapping analysis. However, we could not quantitatively assess this process, because the resulting nitroxides were relatively unstable in the presence of **1b**; increasing concentrations of **1b** impeded the EPR signal of the corresponding spin adducts. To further assess the hydrolysis of **1b** to HNO and •OH, we have applied HPLC protocols that were optimized for quantitative analysis of spin-trapped •OH in the presence of reductants.[13]

In the presence of Fe^{3+} and *N*-methyl-D-glucamine dithiocarbamate (MGD), the hydrolysis of **1b** was paralleled by the appearance of the characteristic EPR spectrum of •ON−Fe^{II}−MGD formed via the interaction of HNO and Fe^{III}−MGD (Figure 1a,b; Scheme 2, **2** → **6**)[14].

The formation of **6** was H^+-independent within the pH interval from 4.0 to 7.4 (Figure 1b), which is in agreement with the findings of Hughes and Cammack that the rate of hydrolysis of **1b** at these proton concentrations is constant. The substitution of Fe^{III}−MGD with 5,5′-dimethyl-1-pyroline *N*-oxide (DMPO) resulted in the appearance of a four-line EPR spectrum with a hyperfine structure (in G) of $a_N = 15.0$ and $a_H = 15.0$, which allowed the assignment of the adduct as that formed by the addition of •OH to DMPO (Figure 1c2; Scheme 2, **4** → **5**).[15] Chelators of metal ions (e.g EDTA (0.1 mM) and desferroxamine (0.1 mM)), catalase (500−2500U/mL), and superoxide dismutase (30−3000 U/mL) did not affect the formation of **5**, suggesting that neither transition metal ions, H_2O_2, nor superoxide anion radical was involved in this production (data not shown). The aerobic hydrolysis of **1** may also lead to the

Scheme 2

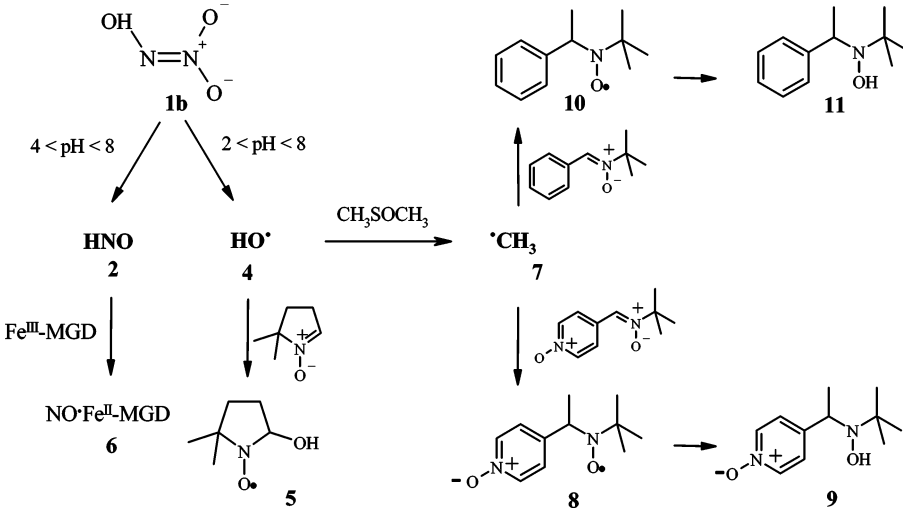

formation peroxynitrite ($ONOO^-$; **12**),[16,17] which may in turn affect EPR spin-trapping measurements.[18] To address this possibility, analogous experiments were carried out under anaerobic conditions. Removal of oxygen from the reaction solutions, however, did not decrease the intensity of the EPR signal from **5**, indicating that $ONOO^-$ did not interfere with the analysis of •OH.[7]

The low stability of nitroxides formed via the interaction of •OH with nitrones is a limiting factor for the quantitation of this species.[19,20] The latter experimental difficulty was solved by the use of dimethyl sulfoxide (DMSO). DMSO is oxidized by •OH to $•CH_3$ (Scheme 2, **4** → **7**), which forms relatively stable nitroxides with α-(4-pyridyl-1-oxide)-*N*-*tert*-butylnitrone (POBN; $•CH_3$ + POBN → **8**) and α-phenyl-*N*-*tert*-butylnitrone (PBN; $•CH_3$ + PBN → **10**). These nitroxides can then be quantified by either EPR or HPLC analysis with electrochemical and/or UV detection.[13]

The hydrolysis of **1b** in the presence of DMSO, PBN, and POBN produced the typical EPR spectra of nitroxides **10** and **8**, respectively (Figure 1c: spectrum 3, a_N = 16.43 G and a_H = 3.59 G; spectrum 4, a_N = 16.01 G and a_H = 2.77 G).[15] The computer-simulated EPR spectra of **5**, **8**, and **10** were in close agreement with the experimental spectra (Figure 1c, trace 5 compared with spectrum 2; trace 6 compared with spectra 3 and 4, respectively). However, both **1b** and HNO can act as reductants,[21,22] implying that the EPR spectra of **5**, **8**, and **10** may not reflect the real amount of •OH and $•CH_3$ formed in the studied system. In the presence of reductants, nitroxides **8** and **10** can be reduced to the corresponding EPR-silent hydroxylamines.[13] In support of the latter assumption, the addition of $K_3[Fe(CN)_6]$ to a solution of **1b**, DMSO, and PBN resulted in a transient increase of the EPR signal of **10**, suggesting the occurrence of an Fe^{III}-dependent oxidation of **11** back to **10** (Figure 1d).

HPLC Analysis of the Hydrolysis of 1. When reaction solutions containing **1b**, DMSO, and either POBN or PBN were analyzed by HPLC with electrochemical and UV detection, respectively, the predominant presence of **9** and **11** was observed (Figure 2a,b). Addition of $K_3[Fe(CN)_6]$ to these solutions resulted in the interconversion of **9** into **8** and **11** into **10**, respectively (data not shown). The identity of compounds **8**−**11** was confirmed by coinjections of authentic HPLC standards, and by EPR analysis of the fractions defined by the corresponding HPLC peaks, as previously described.[13,23] To a first approximation, the formation of **8** plus **9** was 10% of the initial concentration of **1b** (Figure 2c,d). Similar kinetic profiles were observed for the formation of **10** and **11** in solutions containing PBN, DMSO, and **1b**; the overall yield of these adducts was approximately 7% of the initial concentration of **1b** (data not shown). The production of •OH, however, could be higher, as it is unlikely that reactions **1b** → **9** (or **11**) proceeded quantitatively. Furthermore, the production of **9** was unchanged under anaerobic conditions (Figure 2d), implying that the generation of •OH was O_2-independent. In contrast to the hydrolysis of **1b** to HNO, the generation of •OH was strongly affected by the acidity of the reaction solutions (Figure 3a). The latter suggests that the formation of •OH followed the release

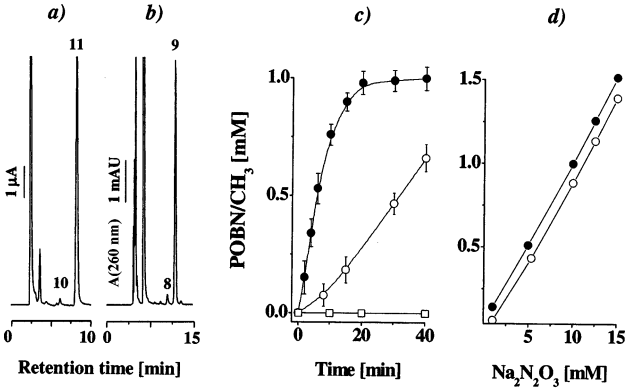

Figure 2. HPLC−EC/UV analysis of **8**−**11** formed in solutions of **1b**. All reactions were carried out in 0.1 M phosphate buffer (pH = 5) for 30 min at 40 °C. DMSO, POBN, and PBN were used at concentrations of 0.2, 0.12, and 0.05 M, respectively. (a) HPLC−EC profile of a reaction solution containing DMSO, PBN, and **1b** (1 mM). (b) HPLC−UV profile of a reaction solution containing DMSO, POBN, and **1b** (1 mM). (c) Kinetics of formation of **9** in solutions containing POBN and DMSO in the absence (□) or in the presence of **1b** (10 mM) at either 25 °C (○) or 40 °C (●). Each experimental point represents the mean of three experiments ± SEM. Kinetics of formation of **9** in solution containing POBN, DMSO, and **1b** in the absence (●) or in the presence (○) of oxygen. Anaerobic conditions were maintained as described in the Experimental Section.

of HNO. Maximal production of •OH was observed within the pH interval from 4 to 6 (Figure 3a), which coincides with the acidity of tumor tissues. At pH = 6.2, the hydrolysis of **1b** to •OH was approximately 10 times higher than that at pH = 7.4.

Effects of pH on the Cytotoxicity of 1b. The pH-dependent production of •OH from **1b** suggests that this compound may exert a H^+-amplified, tissue-specific toxicity. Since cancer cells release protons that create pH gradients with maximal acidity in close proximity to their plasma membranes,[1,24] it is plausible that the H^+-amplified generation of •OH from **1b** will be a process that is more toxic to these cells. To test this hypothesis, we evaluated the cytotoxicity of **1b** at pH values that mimic the microenvironment of normal and tumor tissues, respectively. Figure 4b−d depicts the cytotoxic effect of **1b** on SK-N-SH neuroblastoma cancer cells. A marked increase in the cytotoxicity of **1b** was observed at pH values ranging from 6.2 to 6.8, as compared with pH = 7.0 or 7.4. The toxic effect of **1b** was pronounced several hours after the treatment of the cells. Delayed cell death induced by exposure to oxidative stress has been described in a number of other cell systems and has usually been attributed to apoptosis.[25,26] This cytotoxicity was dependent on the production of •OH, as attested by the protective effect of ascorbic acid (Figure 4d) or POBN and DMSO (50−60% inhibition of the effects of **1b**; data not shown), which are efficient scavengers of radical species. No toxicity was observed when cells were treated with acidic buffers that did not contain **1b** (data not shown).

Acidification of Cancer Cells and Effects of 1b on Tumor Growth in Mice. SK-N-SH neuroblastoma cancer cells (Figure 4a; closed circles) or control HEK (open circles) cells were cultured on 45 mm diameter slides (n = 4 slides for each cell type), labeled with a lectin-conjugated pH indicator dye (WGA-6-carboxy

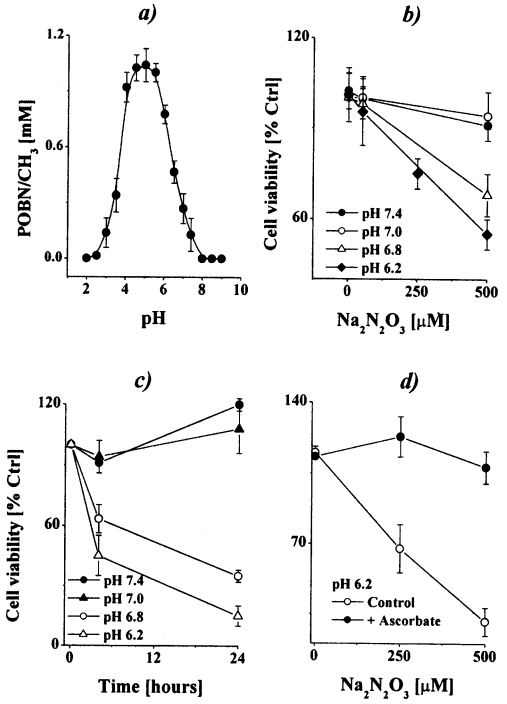

Figure 3. Effects of pH on the hydrolysis and the cytotoxicity of **1b**. Effects of pH on the formation of **9** in 0.1 M phosphate buffers (pH = 2−9) containing DMSO (0.2 M), POBN (50 mM), and **1b** (0.01 M). All reaction solutions were incubated for 30 min at 40 °C. Quantitation of **9** was performed by HPLC−UV with coinjection of 4-methylpicoline as a standard.[13] Each experimental point represents the mean of three experiments ± SEM. (b−d) Effects of proton concentration on the cytotoxicity of **1b**. SK-N-SH neuroblastoma cells (50−100 cells per high-power field) were treated for 30 min at 37 °C with **1b** (panel c, 0.5 mM in 0.050 M phosphate buffer containing 0.15 M NaCl and 0.2 mM $CaCl_2$; pH = 6.2−7.4). Thereafter, the fluid was removed, and the cells were covered with minimal essential medium containing 10% fetal bovine serum and incubated at 37 °C for 4−24 h. In selected experiments, the incubation medium containing **1b** included ascorbic acid (5 mM), superoxide dismutase (300 U per mL), catalase (500 U per mL), and EDTA (0.1 mM; panel d). The cell viability was determined as described in the Experimental Section (n = 4; mean ± SEM expressed as a percentage of the cell count immediately following treatment).

fluorescein) at 4°C for 30 min, and then washed of excess dye. Slides were transferred to the heated stage of an inverted microscope and the dye's fluorescence was found to highlight the membranes with no detectable dye inside or outside the cells. pH from the plasma membrane was then measured ratiometrically (440/480 nm excitation) as a function of time. As shown, the microenvironment of cancer cells became increasingly acidified from a pH of 7.2 to 5.5 over a period of 20 min and then stabilized at pH = 5.5. In contrast, normal HEK cells remained at pH = 7.2−7.4. Each data point represents the mean ± standard deviation from 16 pH recordings (four randomly selected regions of each slide × four slides). In both cell types, the bathing medium was buffered at pH = 7.2 and did not change during the course of the experiment, indicating that the acidification occurred only near the plasma membranes of the cancer cells. The dye's fluorescence was calibrated in another set of experiments by labeling HEK cells and by varying the pH of the bathing medium from 5 to 8. These observations are in agreement with the studies

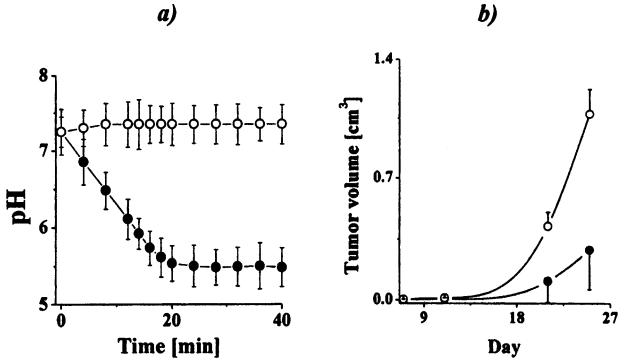

Figure 4. Acidification of cancer cells and effects of **1b** treatment on tumor growth in mice. pH measurements in the microenvironment of SK-N-SH neuroblastoma (solid circles) and control HEK (open circles) cells. Cells were labeled with WGA-6-carboxy fluorescein, as described in the Experimental Section, and covered with 5 mM phosphate buffer, and pH changes on the cells plasma membranes were continuously monitored fluorimetrically at 37 °C. Male NIH athymic mice were injected subcutaneously with PC12 pheochromocytoma cells on day 0 of the study. **1b** (closed circles; 50 mg per kg body weight; n = 4 mice) or vehicle (open circles; n = 4 mice) was administered ip on day 1 and once a week thereafter. The smaller tumor volume in **1b**-treated mice was experimentally significant compared to control group on day 25 with $P < 0.001$ (Student's t test). Each data point represents the mean volume of 16 tumors (four tumors/mice × four).

of Montcourrier et al., who reported that metastatic breast cancer cells from pleural effusions are up to 200-fold more active in acidifying their extracellular milieu than nonmalignant mammary cells cultured under the same conditions.[24] Hence, the acidification of the tumor cells in our experiments was attributed to their higher glycolytic activity compared to the control HEK cells.[1,24] It should be noted, however, that most normal cells do not undergo acidosis under these experimental conditions and could be used as controls instead of HEK cells.

If the pH-dependent conversion of **1b** to •OH is to be viable in the in vivo situation, it must be selectively toxic to tumor cells relative to normal tissues. Hence, experiments were carried out to assess the effects of **1b** on the tumor growth in mice that were injected with neuroblastoma cancer cells. Tumor-bearing mice treated once weekly with 50 mg of **1b** per kg of body weight experienced no apparent toxicity, as evidenced by normal activity and ptosis scores[27,28] throughout the experiment (data not shown; $LD_{50} \sim 220$ mg of **1b** per kg body weight). However, **1b** markedly impeded tumor growth in the group of mice that were injected with **1b** (Figure 4b).

Discussion

In biological systems, nitric oxide (NO•) participates in a complex equilibrium with HNO and metal−nitrosyl complexes that can release nitrosonium NO^+.[29] Elucidation of the multifaceted biological effects of NO• requires characterization of its redox forms as well as the mechanisms of their interconversion. Recent studies have demonstrated that reduction of NO• to HNO leads to distinct cellular responses.[30−32] Unlike NO•, for which there is an extensive and well-established mechanistic and derivative chemistry, our knowledge of HNO is sparse. The latter species is a weak acid whose pK value and redox potential have been recently corrected from

4.7 and −0.3 V to 11.4 and −0.8 V, respectively.[33−35] HNO can be eliminated from various organic molecules; examples are the nitrosative degradation of tertiary amines,[36] the Nef reaction, and prodrugs that can release this species.[37−39] Several groups have reported that **1b**, HNO, and **3**, per se strong reductants, can trigger reactions of oxidation. Mechanistically, these reactions were suggested to occur with the intermediate formation of either •OH [7,9,17,40,41] or (an isomer of)[31] $ONOO^-$.[16,17] Direct detection of the corresponding species, however, has proven to be difficult.

In alkaline solutions, **1** can generate $ONOO^-$ via the intermediate formation of singlet NO^- ($^1NO^-$). Upon relaxation of $^1NO^-$, a triplet state NO^- ($^3NO^-$) is formed that reacts with O_2 to form peroxynitrite.[29,33] However, there are conflicting reports regarding the occurrence of this reaction in acidic-to-neutral solutions. Donald et al. reported that peroxynitrite and its product of decomposition, NO_3^-, are not formed in neutral solutions of **1b**.[29,42] Shafirovich and Lymar have recently pointed out that nitrogen(+1), if formed in biological systems, must be present in the form of ^1HNO ($pK_a = 11.4$). Direct addition of O_2 to ^1HNO, which could yield peroxynitrite, is spin-forbidden and cannot be rapid, if it occurs at all.[33,43] On the other hand, various substrates of peroxynitrite were reported to undergo oxidation in neutral aqueous solutions of **1a** with yields ranging from 1.9% to 65%.[16,17] In control experiments, we observed that Chelex 100 almost completely impeded the consumption of oxygen in solutions of **1b** (Supporting Information). EDTA, in contrast, increased the consumption of oxygen via a mechanism that most likely included the formation of Fe^{III}−EDTA.[44,45] These results suggest that traces of transition metal ions (Me^{n+1}) interacted with HNO to form NO• and Me^{n+};[21,22] in turn, oxidation of Me^{n+} to Me^{n+1} and $O_2^{\bullet-}$ would set the stage for $ONOO^-$ formation. Hence, the HNO-dependent redox cycling of metal ions should be taken into consideration when the interaction of HNO and oxygen is to be assessed.

Hughes et al. reported that in acidic solutions (pH < 3), **1a** decomposes via a free radical chain reaction.[9] Since at pH < 3 the hydrolysis of **1a** leads to the formation of HNO_2 and NO•, esterification of **1a** by HNO_2 was suggested to occur with a concomitant decomposition of the corresponding ester to NO_2, N_2O, and •OH (HO−N═$N^{(+)}O^{(-)}$−OH → ONO−N═$N^{(+)}O^{(-)}$−OH → •OH). Buchholz and Powell proposed a similar mechanism for the formation of •OH in acidic solutions (pH < 3) of **3a** (HO−N═N−OH → ONO−N═N−OH → •OH).[40] However, direct detection of •OH in these reaction systems was not presented. Recently, Wink et al. reported that **1b** is toxic to Chinese hamster V79 lung fibroblast.[46] At a molecular level, **1b** exposure resulted in DNA double-strand breaks in whole cells, suggesting that HNO can act as an oxidant.[46] This observation is in agreement with the studies of Ohshima et al., who reported that HNO produced from **1b** causes DNA strand breakage and base oxidation.[41,47] Scavengers of •OH, metal chelators, superoxide dismutase, and catalase impeded the **1b**-induced oxidation of DNA, implying that superoxide anion radical, H_2O_2, and •OH could be involved in the overall reaction mechanism. On the other hand, **1b** caused oxidation of DNA even under anaerobic conditions,[41] which complicates the elucidation of the exact reaction mechanism.

In this work, we present experimental evidence that in weakly acidified solutions of **1b** both HNO and •OH are formed. In these experiments, the slightly increased formation of •OH under anaerobic conditions was most likely due to an impairment of the competition between POBN and O_2 for $•CH_3$ (Figure 2d; •OH + DMSO → $•CH_3$; $O_2 + •CH_3 → CH_3OO•$). The latter result implies that the generation of •OH was O_2-independent and reflected neither the intermediate formation of $ONOO^-$ nor a redox cycling of transition metal ions. Maximal formation of •OH in solutions of **1b** was observed at pH = 4−5. Hence, •OH was not directly released from **1b** as the formation of HNO within the pH interval of 4−7.5 was H^+-independent (Figure 1b compared to Figure 3a). Since HNO dimerizes to **3**, it could be speculated that this acid partially decomposed to •OH. **3** is a highly unstable compound that is not well-studied. However, its dialkyl esters decompose at room temperature to RO• and N_2,[48] suggesting that the **1b**-dependent formation of •OH reflected the dimerization of HNO to **3** with concomitant azo-type homolytic fission of **3** to N_2 and •OH. Within this mechanism, the effect of H^+ on the formation of •OH can be explained with a shift in the equilibrium between **3** and **3a** in favor of the former (Scheme 1), while the impeded production of •OH at pH < 4 most likely reflected the hydrolysis of **1b** to NO•.[9]

Irrespective of the exact mechanism(s), the generation of •OH from **1b** and/or HNO can have toxicological significance. This generation is well-controlled, occurs under mild conditions, and is markedly affected by small pH variations. With regard to the effects of pH on the **1b**-dependent production of •OH, it is interesting to speculate that this compound may exert tissue-specific toxicity. This production is 1 order of magnitude higher at pH = 6.0 than at pH = 7.4. It could be generalized that metabolic hyperactivity or limited oxygen supply can cause a decrease of tissue pH. Acidosis is characteristic for such disease states as sepsis, arthritis, ischemia, and cancer. In these diseases, the intra- and/or extracellular pH of the affected tissues typically decreases from control values of 7.4 to approximately 6.0.[1,3,49−52] Hence, it is hypothesized that **1b** (and maybe other donors of HNO) can exert selective toxicity to cells subjected to acidosis via a mechanism that includes a pH-dependent, site-specific generation of •OH. In support of this thesis, experimental evidence is presented that **1b** exhibits a pH-dependent cytotoxicity and impedes the growth of tumors in mice. Since **1b** is a hydrophilic compound, it is likely that its toxicological effect(s) were mostly dependent on its extracellular hydrolysis to •OH. The latter assumption, if correct, may explain why the mice experienced no apparent toxicity after receiving consecutive doses of **1b**. It should be noted that in aqueous solutions **1b** maintains low steady-state concentrations of HNO (most likely within the nanomolar range), which could be partially utilized for production of •OH. To the best of our knowledge, there is no literature suggesting that **1b** can exert direct cytotoxicity. Hence, It is tempting to speculate that the in vivo action of **1b** (Figure 4b) reflected a more efficient production of •OH within the acidic microenvironment

of tumor tissues. Further studies are needed, however, to elucidate the conversion of **1b** to HNO and •OH. Understanding these reactions may enhance the mechanistic algorithms to predict the cytotoxicity of prodrugs that release HNO.

Experimental Section

Chemistry. Reagents. Sodium trioxodinitrate was purchased from Calbiochem (San Diego, CA). All other reagents were purchased from Sigma Chem. Co. (St. Louis, MO). The solutions used in the experiments were prepared in deionized and Chelex-100-treated water or potassium phosphate buffer. Sodium trioxodinitrate was either purchased from Calbiochem, Inc. (La Jolla, CA) or synthesized as described in ref 12.

EPR Measurements. EPR spectra were recorded at room temperature on a Bruker ECS106 spectrometer with 50 kHz magnetic field modulation. Computer simulation of the spectra of **5**, **8**, and **10** was performed with hyperfine splitting constants (in G) of $a_N = 14.9$, $a_H = 14.9$; $a_N = 16.10$, $a_H = 2.77$; and $a_N = 16.46$, $a_H = 3.36$, respectively.[15]

HPLC Analysis. HPLC was performed with a Waters Model 510 liquid chromatograph (Milford, MA). Separation was achieved with a C-18 reverse phase column (Microsorb, 4.6 mm × 25 cm, Rainin Instrument Co., Inc., Emeryville, CA). The mobile phase was saturated with helium and contained 10 mM lithium perchlorate and either water with 30% (v/v) methanol for analysis of **8** and **9** or 70% methanol for analysis of **10** and **11**, respectively. All HPLC analyses were conducted at a flow rate of 1 mL per min. Electrochemical detection was carried out at +0.9 V with a LC-4B amperometric system (Bioanalytical Systems, West Lafayette, IN) equipped with glassy carbon electrode and a Ag/AgCl reference electrode. UV detection was carried out within the wavelength range of 200 to 400 nm using an SPD-M10VP Shimadzu diode array detector (Kyoto, Japan).

Preparation of 8−11. Compounds **8** and **10** were prepared as described in ref 13. Briefly, the nitroxide formed after five consecutive additions of 0.02 mL of $Fe(NH_4)(SO_4)_2$ (0.05 M) into a 1 mL solution of a spin-trapping reagent (0.02 M), H_2O_2 (2 mM), EDTA (5 mM), and DMSO (2%) in 0.1 M phosphate buffer (pH = 7.4) was extracted with 2 × 1 mL of ethyl acetate (**8**) or 2 × 1 mL of hexane (**10**). The ethyl acetate (hexane) phase was separated, and the crystals formed after evaporation of the solvent (stream of nitrogen, 25 °C) were redissolved in 1 mL of ethanol and subjected to HPLC purification. The latter was carried out with a mobile phase consisting of either water with 30% (v/v) methanol for separation of **8** and **9** or 70% methanol for separation of **10** and **11**, respectively (column, Econosil C18, 1 cm × 25 cm, Alltech Associates, Deerfield, IL; injection volume, 0.15 mL). An aliquot of the purified **10** or **8** stock solution (0.02 mL) transferred into 0.2 mL phosphate buffer (0.1 M, pH = 7.4) exhibited an EPR spectrum with a triplet of doublets. The hyperfine structure of the EPR spectra was consistent with the data summarized in ref 15 and allowed the assignment of the nitroxides as that formed by addition of $•CH_3$ to POBN and PBN, respectively.

Reduction of both **8** and **10** nitroxides to their hydroxylamine derivatives was performed by incubation of the corresponding nitroxide with ascorbate (10 mM) in 0.1 M phosphate buffer (pH = 7.4; 40 min of incubation at 25 °C). Subsequently, the reaction solution was extracted with ethyl acetate, and the crystals formed after evaporation of the organic solvent (stream of nitrogen; 25 °C) were redissolved in ethanol. The ethanolic solutions obtained did not exhibit the typical EPR spectra of **8** and **10**, which were observed before the incubation with ascorbate. The identities of the hydroxylamine derivatives were confirmed by GC−MS analysis as described in ref 23. Compounds **8**−**11** were stable for several months when stored in ethanol at −20 °C.

Anaerobic Experiments. To achieve anaerobic conditions, all solutions were placed in septum-caped vials and purged for 45 min with a stream of nitrogen. Thereafter, additions to the final reaction solutions were made through the septum of the corresponding vial using a 0.10 mL gastight syringe.

Pharmacology. Measurements of Extracellular pH. SK-N-SH neuroblastoma cells (Figure 4a; closed circles) or control HEK (open circles) cells were cultured on 45 mm diameter slides ($n = 4$ slides for each cell type), labeled with a lectin-conjugated pH indicator dye (WGA-6-carboxy fluorescein, 2 μM; Molecular Probes, OR) at 4 °C for 30 min and then washed of excess dye with 5 mM phosphate buffer. Slides were transferred to the heated stage of an inverted Nikon microscope and the dye's fluorescence was found to highlight the membranes with no detectable dye inside or outside the cells. pH from the plasma membrane was then measured ratiometrically as a function of time ($\lambda_{ex} = 440/480$; and $\lambda_{em} = 505$ nm). The dye's fluorescence was calibrated in another set of experiments by labeling HEK cells and by varying the pH of the bathing medium (5 mM phosphate buffer) from 5 to 8.

Cell Experiments. The cytotoxic effect of **1b** on SK-N-SH neuroblastoma cells was assessed with the cell titer 96 nonradioactive cell proliferation assay kit (Promega, Madison WI). Cells (800−1000) were seeded onto 24-well plates and incubated with 0.1 M phosphate buffer (pH = 4−7.5; ΔpH = 0.2) containing 150 mM NaCl, 0.2 mM $CaCl_2$, and different concentrations of **1b** (0.05−0.5 mM) for 30 min. Thereafter, the fluid was removed, and the cells were covered with MEM containing 10% fetal bovine serum and incubated at 37 °C for 4, 8, 12, and 24 h. After addition of the "stop" solution, the absorbance of the reaction solution at 570 nm was recorded. The absorbance at 630 nm was used as reference. The net $A_{570} - A_{630}$ was taken as the index of cell viability. The net absorbance from the wells of cells cultured with control medium was taken as the 100% viability value. The percentage of viability of the treated cells was calculated by the formula $(A_{570} - A_{630})_{sample}/(A_{570} - A_{630})_{control} \times 100$.

Mice Experiments. Experiments involving tumor growth were performed on 5−7 week-old male NIH athymic mice injected subcutaneously with 10^7 SK-N-SH neuroblastoma cells into the left flank on day 0 of each study. For studies mimicking minimal residual disease (a frequent clinical presentation after surgery for neuroblastoma), **1b** (50 mg/kg body weight) was administered intraperitoneally once daily on days 1, 7, 14, and 28 ($n = 4$ mice). The control group ($n = 4$ mice) consisted of mice injected with the same batch and volume of SK-N-SH neuroblastoma cells that were then treated on days 1, 7, 14, and 28 with an injection of the vehicle [50 mM phosphate buffer (pH = 6.2−7.4) containing 0.15 M NaCl and 0.2 mM $CaCl_2$ but no **1b**]. Mice were examined daily for grossly visible tumor, and once tumors appeared, their size was assessed by measuring the largest and smallest diameters of each tumor at multiple time points during the month following implantation. Tumor volume was calculated as the product of the largest diameter and the square of the smallest diameter. Mean tumor volume for the four mice in each group was calculated for each day of tumor measurement, assuming a tumor volume of 0 for those mice in which a tumor was not palpable. Statistical significance of differences in mean tumor volume was determined for each day's measurements using Student's *t* test. In Figure 4b, each data point was the mean tumor volume of 16 tumors (four tumors/mice × four mice).

Acknowledgment. These studies were supported by U. S. Public Health Service Grant ES09648 from The National Institute for Environmental Health Sciences (D.A.S.) and a grant from PhroCure LLC (N.F.S.).

Supporting Information Available: Figure depicting the consumption of oxygen in aqueous solutions of **1b**. This material is available free of charge via the Internet at http://pubs.acs.org.

References

(1) Stubbs, M.; McSheehy, P. M.; Griffiths, J. R.; Bashford, C. L. Causes and consequences of tumour acidity and implications for treatment. *Mol. Med. Today* **2000**, *6*, 15−19.

(2) Vaupel, P.; Okunieff, P.; Neuringer, L. J. Blood flow, tissue oxygenation, pH distribution, and energy metabolism of murine mammary adenocarcinomas during growth. *Adv. Exp. Med. Biol.* **1989**, *248*, 835−845.
(3) Vaupel, P. W.; Frinak, S.; Bicher, H. I. Heterogeneous oxygen partial pressure and pH distribution in C3H mouse mammary adenocarcinoma. *Cancer Res.* **1981**, *41*, 2008−2013.
(4) Jahde, E.; Glusenkamp, K. H.; Rajewsky, M. F. Nigericin enhances mafosfamide cytotoxicity at low extracellular pH. *Cancer Chemother. Pharmacol.* **1991**, *27*, 440−444.
(5) Raghunand, N.; Mahoney, B.; van Sluis, R.; Baggett, B.; Gillies, R. J. Acute metabolic alkalosis enhances response of C3H mouse mammary tumors to the weak base mitoxantrone. *Neoplasia* **2001**, *3*, 227−235.
(6) Gerweck, L. E. Tumor pH: Implications for treatment and novel drug design. *Semin. Radiat. Oncol.* **1998**, *8*, 176−182.
(7) Stoyanovsky, D. A.; Clancy, R. M.; Cederbaum, A. I. Decomposition of Sodium Trioxodinitrate (Angeli's Salt) to Hydroxyl Radical: An ESR Spin-Trapping Study. *J. Am. Chem. Soc.* **1999**, *121*, 5093−5094.
(8) Halliwell, B.; Gutteridge, J. M. Role of free radicals and catalytic metal ions in human disease: An overview. *Methods Enzymol.* **1990**, *186*, 1−85.
(9) Hughes, M. N.; Wimbledon, P. E. The chemistry of trioxodinitrates. Part I. Decomposition of sodium trioxodinitrate (Angeli's salt) in aqueous solution. *J. Chem. Soc., Dalton* **1976**, 703−707.
(10) Bonner, F. T.; Ravid, B. Thermal decomposition of oxyhyponitrite (Sodium trioxodinitrate(II) in aqueous solutions. *J. Inorg. Chem.* **1975**, *14*, 558−563.
(11) Loechler, E. L.; Schneider, A. M.; Schwartz, D. B.; Hollocher, T. C. Covalent electrophilic catalysis of the breakdown of hyponitrite to nitrous oxide by aldehydes, ketones, and carbon dioxide. *J. Am. Chem. Soc.* **1987**, *109*, 3076−3087.
(12) Smith, P. A. S.; Hein, G. E. The alleged role of nitroxyl in certain reactions of aldehyde and alkyl halides. *J. Am. Chem. Soc.* **1960**, *82*, 5731−5740.
(13) Stoyanovsky, D. A.; Melnikov, Z.; Cederbaum, A. I. ESR and HPLC-EC analysis of the interaction of hydroxyl radical with DMSO: Rapid reduction and quantification of POBN and PBN nitroxides. *Anal. Chem.* **1999**, *71*, 715−721.
(14) Xia, Y.; Cardounel, A. J.; Vanin, A. F.; Zweier, J. L. Electron paramagnetic resonance spectroscopy with *N*-methyl-D-glucamine dithiocarbamate iron complexes distinguishes nitric oxide and nitroxyl anion in a redox-dependent manner: Applications in identifying nitrogen monoxide products from nitric oxide synthase. *Free Radic. Biol. Med.* **2000**, *29*, 793−797.
(15) Buettner, G. R. Spin trapping: ESR parameters of spin adducts. *Free Radic. Biol. Med.* **1987**, *3*, 259−303.
(16) Vanuffelen, B. E.; Van Der Zee, J.; De Koster, B. M.; Vansteveninck, J.; Elferink, J. G. Intracellular but not extracellular conversion of nitroxyl anion into nitric oxide leads to stimulation of human neutrophil migration. *Biochem. J.* **1998**, *330* (Pt 2), 719−722.
(17) Kirsch, M.; de Groot, H. Formation of peroxynitrite from reaction of nitroxyl anion with molecular oxygen. *J. Biol. Chem.* **2002**, *277*, 13379−13388.
(18) Gatti, R. M.; Alvarez, B.; Vasquez-Vivar, J.; Radi, R.; Augusto, O. Formation of spin trap adducts during the decomposition of peroxynitrite. *Arch. Biochem. Biophys.* **1998**, *349*, 36−46.
(19) Towell, J.; Kalyanaraman, B. Detection of radical adducts of 5,5-dimethyl-1-pyrroline n-oxide by the combined use of high-performance liquid chromatography with electrochemical detection and electron spin resonance. *Anal. Biochem.* **1991**, *196*, 111−119.
(20) Janzen, E. G.; Kotake, Y.; Hinton, R. D. Stabilities of hydroxyl radical spin adducts of PBN-type spin traps. *Free Radic. Biol. Med.* **1992**, *12*, 169−173.
(21) Al-Ajlouni, A. M.; Gould, E. S. Electron transfer. 139. Reductions with trioxodinitrate, N_2O_3 (2-). *Inorg. Chem.* **1999**, *38*, 1592−1595.
(22) Nelli, S.; Hillen, M.; Buyukafsar, K.; Martin, W. Oxidation of nitroxyl anion to nitric oxide by copper ions. *Br. J. Pharmacol.* **2000**, *131*, 356−362.
(23) Novakov, C. P.; Feierman, D.; Cederbaum, A. I.; Stoyanovsky, D. A. An ESR and HPLC-EC assay for the detection of alkyl radicals. *Chem. Res. Toxicol.* **2001**, *14*, 1239−1246.
(24) Montcourrier, P.; Silver, I.; Farnoud, R.; Bird, I.; Rochefort, H. Breast cancer cells have a high capacity to acidify extracellular milieu by a dual mechanism. *Clin. Exp. Metastasis* **1997**, *15*, 382−392.
(25) Hockenbery, D. M.; Oltvai, Z. N.; Yin, X. M.; Milliman, C. L.; Korsmeyer, S. J. Bcl-2 functions in an antioxidant pathway to prevent apoptosis. *Cell* **1993**, *75*, 241−251.
(26) Pierce, G. B.; Parchment, R. E.; Lewellyn, A. L. Hydrogen peroxide as a mediator of programmed cell death in the blastocyst. *Differentiation* **1991**, *46*, 181−186.
(27) Purpura, P.; Westman, L.; Will, P.; Eidelman, A.; Kagan, V. E.; Osipov, A. N.; Schor, N. F. Adjunctive treatment of murine neuroblastoma with 6-hydroxydopamine and Tempol. *Cancer Res.* **1996**, *56*, 2336−2342.
(28) Schor, N. F. T. Adjunctive use of Ethiofos (WR2721) with free radical-generating chemotherapeutic agents in mice: New caveats for therapy. *Cancer Res.* **1987**, *47*, 5411−5414.
(29) Hughes, M. N. Relationships between nitric oxide, nitroxyl ion, nitrosonium cation and peroxynitrite. *Biochim. Biophys. Acta* **1999**, *1411*, 263−272.
(30) Ma, X. L.; Gao, F.; Liu, G. L.; Lopez, B. L.; Christopher, T. A.; Fukuto, J. M.; Wink, D. A.; Feelisch, M. Opposite effects of nitric oxide and nitroxyl on postischemic myocardial injury. *Proc. Natl. Acad. Sci. U.S.A.* **1999**, *96*, 14617−14622.
(31) Miranda, K. M.; Espey, M. G.; Yamada, K.; Krishna, M.; Ludwick, N.; Kim, S.; Jourd'heuil, D.; Grisham, M. B.; Feelisch, M.; Fukuto, J. M.; Wink, D. A. Unique oxidative mechanisms for the reactive nitrogen oxide species, nitroxyl anion. *J. Biol. Chem.* **2001**, *276*, 1720−1727.
(32) Paolocci, N.; Katori, T.; Champion, H. C.; St John, M. E.; Miranda, K. M.; Fukuto, J. M.; Wink, D. A.; Kass, D. A. Positive inotropic and lusitropic effects of HNO/NO^- in failing hearts: Independence from beta-adrenergic signaling. *Proc. Natl. Acad. Sci. U.S.A.* **2003**, *100*, 5537−5542.
(33) Shafirovich, V.; Lymar, S. V. Nitroxyl and its anion in aqueous solutions: Spin states, protic equilibria, and reactivities toward oxygen and nitric oxide. *Proc. Natl. Acad. Sci. U.S.A.* **2002**, *99*, 7340−7345.
(34) Bartberger, M. D.; Fukuto, J. M.; Houk, K. N. On the acidity and reactivity of HNO in aqueous solution and biological systems. *Proc. Natl. Acad. Sci. U.S.A.* **2001**, *98*, 2194−2198.
(35) Bartberger, M. D.; Liu, W.; Ford, E.; Miranda, K. M.; Switzer, C.; Fukuto, J. M.; Farmer, P. J.; Wink, D. A.; Houk, K. N. The reduction potential of nitric oxide (NO) and its importance to NO biochemistry. *Proc. Natl. Acad. Sci. U.S.A.* **2002**, *99*, 10958−10963.
(36) Smith, P. A. S.; Pars, H. G. Nitrosative cleavage of *N′*,*N′*-dialkylhydrazides and tertiary amines. *J. Org. Chem.* **1959**, *24*, 1325−1328.
(37) Nagasawa, H. T.; Kawle, S. P.; Elberling, J. A.; DeMaster, E. G.; Fukuto, J. M. Prodrugs of nitroxyl as potential aldehyde dehydrogenase inhibitors vis-à-vis vascular smooth muscle relaxants. *J. Med. Chem.* **1995**, *38*, 1865−1871.
(38) Lee, M. J.; Shoeman, D. W.; Goon, D. J.; Nagasawa, H. T. N-hydroxybenzenecarboximidic acid derivatives: A new class of nitroxyl-generating prodrugs. *Nitric Oxide* **2001**, *5*, 278−287.
(39) Conway, T. T.; DeMaster, E. G.; Lee, M. J.; Nagasawa, H. T. Prodrugs of nitroxyl and nitrosobenzene as cascade latentiated inhibitors of aldehyde dehydrogenase. *J. Med. Chem.* **1998**, *41*, 2903−2909.
(40) Buchholz, J. R.; Powell, R. E. The decomposition of hyponitrous acid: II. The chain reaction. *J. Am. Chem. Soc.* **1965**, *87*, 2350−2353.
(41) Ohshima, H.; Gilibert, I.; Bianchini, F. Induction of DNA strand breakage and base oxidation by nitroxyl anion through hydroxyl radical production. *Free Radic. Biol. Med.* **1999**, *26*, 1305−1313.
(42) Donald, C. E.; Hughes, M. N.; Thompson, J. M.; Bonner, F. T. Photolysis of the nitrogen−nitrogen double bond in trioxodinitrate: Reaction between triplet oxonitrate(1−) and molecular oxygen to form peroxonitrite. *Inorg. Chem.* **1986**, *25*, 2676−2677.
(43) Shafirovich, V.; Lymar, S. V. Spin-forbidden deprotonation of aqueous nitroxyl (HNO). *J. Am. Chem. Soc.* **2003**, *125*, 6547−6552.
(44) Welch, K. D.; Davis, T. Z.; Aust, S. D. Iron autoxidation and free radical generation: Effects of buffers, ligands, and chelators. *Arch. Biochem. Biophys.* **2002**, *397*, 360−369.
(45) Rashba-Step, J.; Turro, N. J.; Cederbaum, A. I. ESR studies on the production of reactive oxygen intermediates by rat liver microsomes in the presence of NADPH or NADH. *Arch. Biochem. Biophys.* **1993**, *300*, 391−400.
(46) Wink, D. A.; Feelisch, M.; Fukuto, J.; Chistodoulou, D.; Jourd'heuil, D.; Grisham, M. B.; Vodovotz, Y.; Cook, J. A.; Krishna, M.; DeGraff, W. G.; Kim, S.; Gamson, J.; Mitchell, J. B. The cytotoxicity of nitroxyl: Possible implications for the pathophysiological role of NO. *Arch. Biochem. Biophys.* **1998**, *351*, 66−74.
(47) Ohshima, H.; Yoshie, Y.; Auriol, S.; Gilibert, I. Antioxidant and pro-oxidant actions of flavonoids: Effects on DNA damage induced by nitric oxide, peroxynitrite and nitroxyl anion. *Free Radic. Biol. Med.* **1998**, *25*, 1057−1065.
(48) Paul, T.; Ingold, K. U. A method for thermal generation of aryloxyl radicals at ambient temperatures: Application to low-density lipoprotein (LDL) oxidation. *Angew. Chem., Int. Ed. Engl.* **2002**, *41*, 804−806.
(49) Jacobi, J. Pathophysiology of sepsis. *Am. J. Health Syst. Pharm.* **2002**, *59 Suppl 1*, S3−8.

(50) Andersson, S. E.; Lexmuller, K.; Johansson, A.; Ekstrom, G. M. Tissue and intracellular pH in normal periarticular soft tissue and during different phases of antigen induced arthritis in the rat. *J. Rheumatol.* **1999**, *26*, 2018−2024.
(51) Gasbarrini, A.; Borle, A. B.; Farghali, H.; Francavilla, A.; Van Thiel, D. Fructose protects rat hepatocytes from anoxic injury. Effect on intracellular ATP, Ca2+i, Mg2+i, Na+i, and pHi. *J. Biol. Chem.* **1992**, *267*, 7545−7552.
(52) Owens, L. M.; Fralix, T. A.; Murphy, E.; Cascio, W. E.; Gettes, L. S. Correlation of ischemia-induced extracellular and intracellular ion changes to cell-to-cell electrical uncoupling in isolated blood-perfused rabbit hearts. Experimental Working Group. *Circulation* **1996**, *94*, 10−13.

JM030192J